J Mol Model (2012) 18:3821–3830
DOI 10.1007/s00894-012-1376-5

ORIGINAL PAPER

The degradation mechanism of phenol induced by ozone in wastes system

Sun Youmin · Ren Xiaohua · Cui Zhaojie · Zhang Guiqin

Received: 28 June 2011 / Accepted: 6 February 2012 / Published online: 9 March 2012

Abstract A distinct understanding for the degradation mechanism of phenol induced by ozone is very essential because the ozonation process, one of the advanced oxidation processes (AOPs), is attractive and popular in wastewater treatment. In the present work, the detailed reactions of ozone and phenol are investigated employing the density functional theory B3LYP method with the 6-311++G (d, p) basis set. The profiles of the potential energy surface are constructed and the possible reaction pathways are indicated. These detailed calculation results suggest two degradation reaction mechanisms. One is phenolic H atom abstraction mechanism, and the other is cyclo-addition and ring-opening mechanism. Considering the effect of solvent water, the calculated energy barriers and reaction enthalpies for the reaction of O3 and phenol in water phase are both lower than those in gas phase, though the degradation mechanisms are not changed. This reveals that these degradation reactions are more favorable in the water solvent. The main reaction products are $C_6H_5OO\cdot$ radical, a crucial precursor for forming PCDD/Fs and one ring-opening product, which are in good agreement with the experimental observations.

Keywords Degradation mechanism · Density functional theory · Ozonation · Phenol

Introduction

Phenolic compounds are generally produced in the petrochemical, pesticide manufacture, coal conversion process, additives and aromatic chemical, dye and pharmaceutical industries and so on [1–6]. They are all toxic organic contaminants, and serious environmental risks and pollutions are generated when they are discharged into water. They are strongly harmful to aquatic life and human health even at concentrations in the parts per billion range, and they impart a disgusting odor [3, 7]. Of these, phenol is classified as a priority pollutant in the list of United States Environmental Protection Agency (USEPA) for its toxic, carcinogenic, mutagenic, teratogenic and non-biodegradable properties [8]. Therefore, intensive attention has been paid to remove phenolic compounds from wastewater, and treatment technologies available are physical, chemical, biological processes and so on [9–11]. Among these choices, advanced oxidation processes (AOPs) which can completely mineralize organic pollutants are probably the best option in treating such wastewater [12, 13]. These processes mainly involve direct ozonization, ozone in combination with UV, hydrogen peroxide oxidation, ozone plus hydrogen peroxide (O_3/H_2O_2), UV photolysis, Fenton's reagent and photocatalysis, etc. [6, 14–18]. As one of the most attractive oxidizing agents, ozone is widely used for disinfecting drinking water and oxidizing various organic contaminants in industrial wastewaters [19]. In the water system, ozone is unstable and can decompose into ·OH radicals. Therefore, ozone can play an important role via a direct reaction pathway involving molecular ozone or an

S. Youmin · R. Xiaohua · C. Zhaojie (✉)
School of Environmental Science and Engineering, Shandong University, Jinan 250100, People's Republic of China
e-mail: cuizj@sdu.edu.cn

S. Youmin · Z. Guiqin
School of Municipal and Environmental Engineering, Shandong Jianzhu University, Jinan 250101, People's Republic of China

indirect pathway involving ·OH radicals to degrade organic pollutants in wastewater treatment [20].

The simple phenol was investigated most frequently as a model pollutant for other phenols and organic compounds containing activated phenol rings in past studies [9, 21]. The experimental results of Ning Bo et al. [22] revealed that alkyl-chain plays a minor role during the reaction of ozone and phenol with alkyl-chain. So, we take phenol as an example in the present work. As for phenol, a great deal of researches on the oxidizing mechanism by ·OH radical has been carried out experimentally and theoretically [13, 21, 23–26]. And the H-atom abstraction and addition mechanisms have almost been clarified. Moreover, some experimental and theoretical research on the ozonation of the substituted hydrazines show that the reactions are abstracting both aliphatic and aromatic hydrogen and adding to the unsaturated double bonds [27]. However, phenol is different because of the carbon-carbon bonds in the ring of phenol unlike the ordinary unsaturated double bonds.

The study for the reaction mechanism of O_3 and phenol mainly focused on laboratory experiments, and possible reaction pathways were proposed based on the data [6, 28–31]. However, the detailed reaction mechanism of ozone abstracting phenolic H atom and adding to the benzene ring of phenol has not been clarified clearly. In addition, studying the destruction mechanism of phenol by ozone is crucial to improve the understanding for the degradation of its derivatives such as chlorophenols, phenoxy herbicides and so on. Moreover, quantum chemistry calculation is especially favorable for establishing the feasibility of reaction paths [32]. Therefore, a thorough study of O_3 abstracting phenolic H atom from phenol and adding to the carbon-carbon bonds of phenol is undertaken using the quantum chemical method. Moreover, the pathways and intermediates of phenol degradation under ozonation are identified.

Computational details

Theoretical calculations are carried out in the framework of DFT using GAUSSIAN 03 program package [33]. The choice of the basis sets and levels is considered on the basis of the computational accuracy and feasibility as well as economical computational time [34, 35]. All geometrical parameters of reactants, intermediates, transition states and products are optimized at the B3LYP [36, 37] level with a standard 6-311++G (d, p) basis set. In addition, all structures involved in the reaction have been located on the potential energy surface (PES) by performing full geometry optimization without any symmetry restriction, and their natures (local minima or first-order saddle points), the zero point energies (ZPEs) and thermal contributions to the total energy have been identified by performing frequency calculations, and all transition states are characterized by one negative eigenvalue and verified to connect the designated reactants with products by employing intrinsic reaction coordinate (IRC) [38, 39] calculations. In the present study, the effect of solvent water using the polarizable continuum model (PCM) is taken into account and the solvation structures involved in the reactions of ozone and phenol is all optimized with the B3LYP/6-311++G (d, p) method. For all energies, the ZPE corrections have been included.

Results and discussion

Figure 1 displays the structure and atom labels of phenol. The molecular structure proposed as well as calculated HOMO and LUMO of ozone are shown in Fig. 2.

The property of ozone molecular

With respect to the electronic structure and geometry of ozone, there are several different theories proposed by researchers. Pauling [40] developed the resonance theory by two equal weighting structures (Fig. 1a). Three main coexisting structures of ozone proposed by Weinhold [41] are presented in Fig. 2b. Moreover, the structure of three-electron bonding for ozone proposed by Linnett [42] displays that singlet biradical character on two terminal oxygens, which explains the fact that ozone generally adds into the unsaturated bonds using the two terminal atoms.

As illustrated in Table 1 and Fig. 2d, the electronic structure of O_3 we calculated is identical with the result of Pakiari [43]. The calculated result displays that ozone is a bent geometry with inner-bond angle of 118.4° and bond length of 1.256 Å.

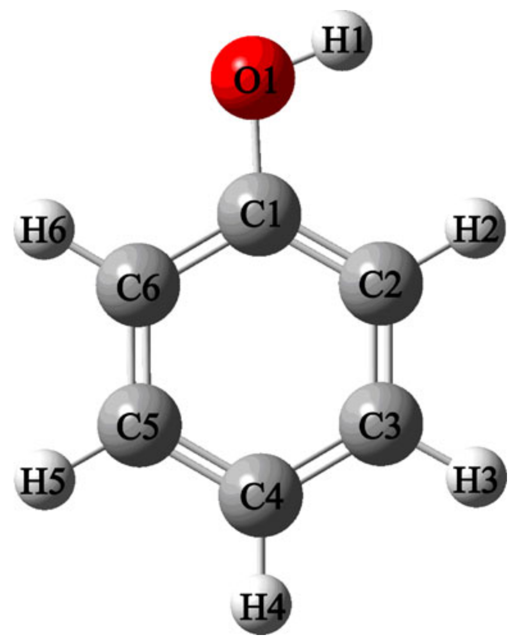

Fig. 1 The structure of phenol

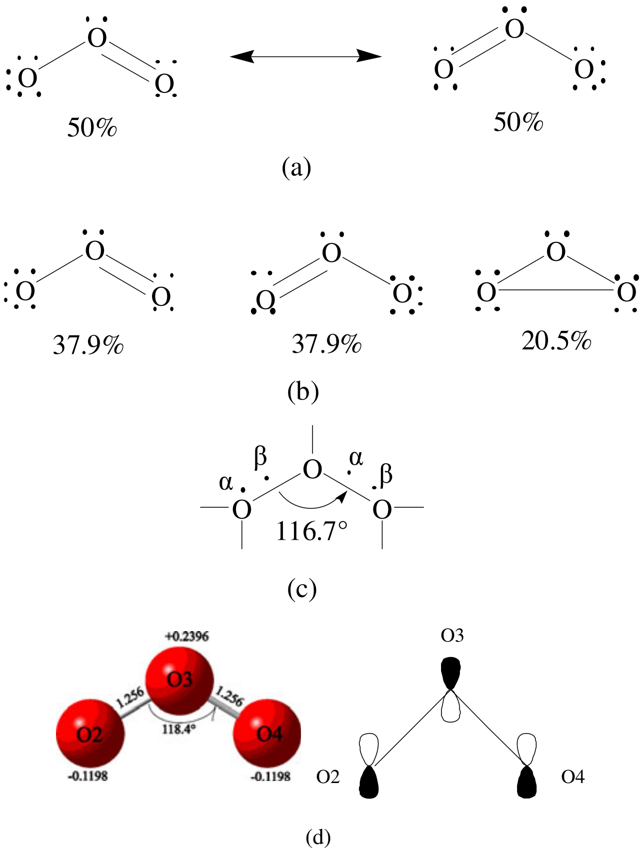

Fig. 2 The structure as well as HOMO and LUMO of ozone (**a**) by Pauling's resonance theory; (**b**) by Weinhold's resonance theory (NRT); (**c**) by Linnett's double quartet theory; (**d**) by B3LYP/6-311++G(d,p)

Also, Pakiari [43] obtains that the bond orders of O2-O3 and O3-O4 are both about 2, indicating that these two bonds are double bond. Seen from the frontier orbital analysis of ozone, the eigenvectors of HOMO and LUMO for the two terminal oxygen atoms are the same and opposed to that of the central oxygen. The orbital energy of LUMO of ozone is -0.2044 Hartree. Additionally, the calculated orbital energy of HOMO of reaction phenol is -0.2344 Hatree and the difference between them is 0.030 Hartree. According to the molecular orbital theory by Fukui [44, 45], they can react easily. Theoretical orbital analysis can well explain the experimental ozone treatment technique in the advanced oxidation processes [12, 13].

Table 1 Calculated eigenvalues and eigenvectors of HOMO and LUMO of O_3

Eigenvalues	HOMO		LUMO	
E/Hartree	−0.3548		−0.2044	
Atoms	Eigenvectors		Eigenvectors	
O3	2Pz	−0.138	2Px	0.226
	3Pz	−0.201	3Px	0.332
	4Pz	−0.138	4Px	0.333
	5Pz	−0.016	5Px	0.095
O2	2Pz	0.209	2Px	−0.193
	3Pz	0.308	3Px	−0.282
	4Pz	0.278	4Px	−0.292
	5Pz	0.042	5Px	−0.097
O4	2Pz	0.209	2Px	−0.193
	3Pz	0.308	3Px	−0.282
	4Pz	0.278	4Px	−0.292
	5Pz	0.042	5Px	−0.097

Bond dissociation enthalpy (BDE)

Bond dissociation enthalpy (BDE) is a good thermodynamic parameter for predicting the strength of the chemical H-X bond of organic compounds [46]. To estimate which are the vulnerable bonds of phenol, the O-H and C-H BDEs are both calculated according to the defined of the reaction enthalpy at 298 K and 1 atm [44], in which the thermal corrections to the enthalpy is also considered. The detailed Eq. (1) used to obtain the O-H BDE for the O-H bond of phenol at 298 K and 1 atm is as follows [46]:

$$\mathrm{BDE(A-H)} = \Delta_f H^{298}_{A^\cdot} + \Delta_f H^{298}_{H^\cdot} - \Delta_f H^{298}_{A-H}, \tag{1}$$

where $\Delta_f H^{298}_{A^\cdot}$, $\Delta_f H^{298}_{H^\cdot}$, $\Delta_f H^{298}_{A-H}$ are the heats of formation of the radicals A and H and the molecule A-H, respectively. To obtain a more reliable and accurate value of BDE, the B3P86/6-311++G (d, p) method is carried out for the single-point energy calculations on the optimization structure with the B3LYP/6-311++G (d, p) level. The calculated results are shown in Table 2. From Table 2, it can be seen that the calculated BDE for the O1-H bond of 86.9 kcal·mol^{-1} is the lowest, which is consistent with the experimental BDE (O-H) of 86.2 kcal·mol-1 [47]. Besides, the calculated similar larger BDEs values of around 110 kcal·mol^{-1} for all the C-H bonds prove that they are harder to be dissociated. Therefore, the O1-H bond is indicated to be the easiest to cleavage, which is in agreement with early research [48–51].

O3-initiated degradation mechanism

The possible pathways for the reactions of O_3 and phenol are presented in Scheme 1. $\cdot O_3H$ radical, a crucially unstable

Table 2 Calculated C-H and O-H bond dissociation enthalpies of phenol at the B3P86/6-311++G(d,p)//B3LYP/6-311++G(d,p) level and temperature 298.15 K

Bond position	Bond dissociation enthalpies (kcal·mol^{-1})
O1-H	86.9
C2-H	112.6
C3-H	112.2
C4-H	113.4
C5-H	112.2
C6-H	114.4

intermediate during the ozonization of phenol [29, 52], still possess the capability of oxidizing organic pollutants. So the pathways for the $\cdot O_3H$ radical and phenol reactions are also considered as shown in Scheme 2. The optimized geometries including the various intermediates and transition states involved in the reactions are displayed in Fig. 3. The profiles of the potential energy surface with the zero-point energy (ZPE) correction are depicted in Figs. 4, 5 and 6, and the relevant energies are given in Table 3.

H-atom abstraction mechanism

According to the analyses of the calculated static parameters above, it can be conjectured that the O1-H bond is the most vulnerable bond to be broken. So the phenolic H abstraction reactions are first considered. We find three pathways denoted R1-3 for the H abstraction reaction of O_3 and phenol, in which O_3 abstracts the phenolic H with different orientations. Also, there exist two pathways for the reaction of $\cdot O_3H$ radical abstracting phenolic H, denoted R7 and R8. In the three pathways of O_3 abstracting phenolic H, three H-bonded pre-complexes, IM1、IM3 and IM5, are first formed, which are slightly more stable than the separate reactants (2.17 kcal·mol^{-1} for IM1, 1.85 kcal·mol^{-1} for IM3 and 2.82 kcal·mol^{-1} for IM5) because of the stabilization of three O2…H1O1 hydrogen bonds in them. Along the pathway R1, IM1 is converted to IM2 via transition state TS1 with an activation energy of 14.53 kcal·mol^{-1}, and the overall reaction is slightly exothermic by 7.29 kcal·mol^{-1}. The elongation of the bond being broken and the bond being formed with regard to the equilibrium value in the reactants and products is the most important character of the transition state [52]. In the TS1 structure, the O1-H1 bond being broken is elongated by 46.23% compared to IM1, while the O2-H1 bond being formed is slightly longer than the value 0.972 Å in

Scheme 2 Possible pathways for abstracting H from phenol by $\cdot O_3H$

IM2 by 9.98%. Then $C_6H_5O\cdot$ radical (denoted P1) and $\cdot O_3H$ radical are produced due to the decomposition of IM2. This process is consistent with the result by Denisova et al. [53]. $C_6H_5O\cdot$ radical is the main intermediate during the reaction of phenol and ozone. $C_6H_5O\cdot$ radical has a resonance structure, and the radical character is localized on the phenolic oxygen, as well as on the para- and ortho-carbons through delocalization [54]. The association reactions of the phenoxy radicals through these radical sites yield six different dimers, which can also convert between each other [55–57]. Both the dimers and their interconversions can form PCDD/Fs with lower or no activation barriers [57, 58]. Therefore, identifying the intermediate $C_6H_5O\cdot$ radical is very important so that we can take preventive measures to avoid generating it or add other chemical reagents to react with it. In addition, $\cdot O_3H$ radical is also formed and can abstract a second H atom from phenol, which is discussed later.

The R2 path proceeds via transition state TS2 with an energy barrier of 12.31 kcal·mol^{-1}, and then an adduct IM4 with high reaction energy of 23.85 kcal·mol^{-1} is formed. The decomposition of IM4 produces $\cdot HO_2$ radical, which is still highly reactive and can react with phenol, and p-$C_6H_5OO\cdot$ radical (denoted as P2), which can be transformed into p-bezenoquinone by further oxidizing. The whole reaction is exothermic by 8.57 kcal·mol^{-1}.

There is a transition state TS3 identified along the reaction R3 with a potential barrier of 6.19 kcal·mol^{-1}, which is the lowest energy of all three abstracting reactions. Thus, this process

Scheme 1 Possible pathways for the reaction of O_3 and phenol

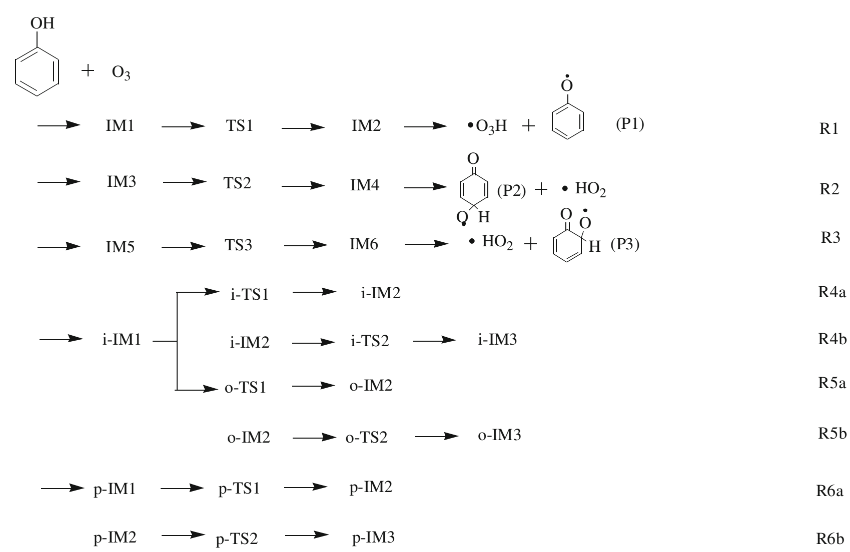

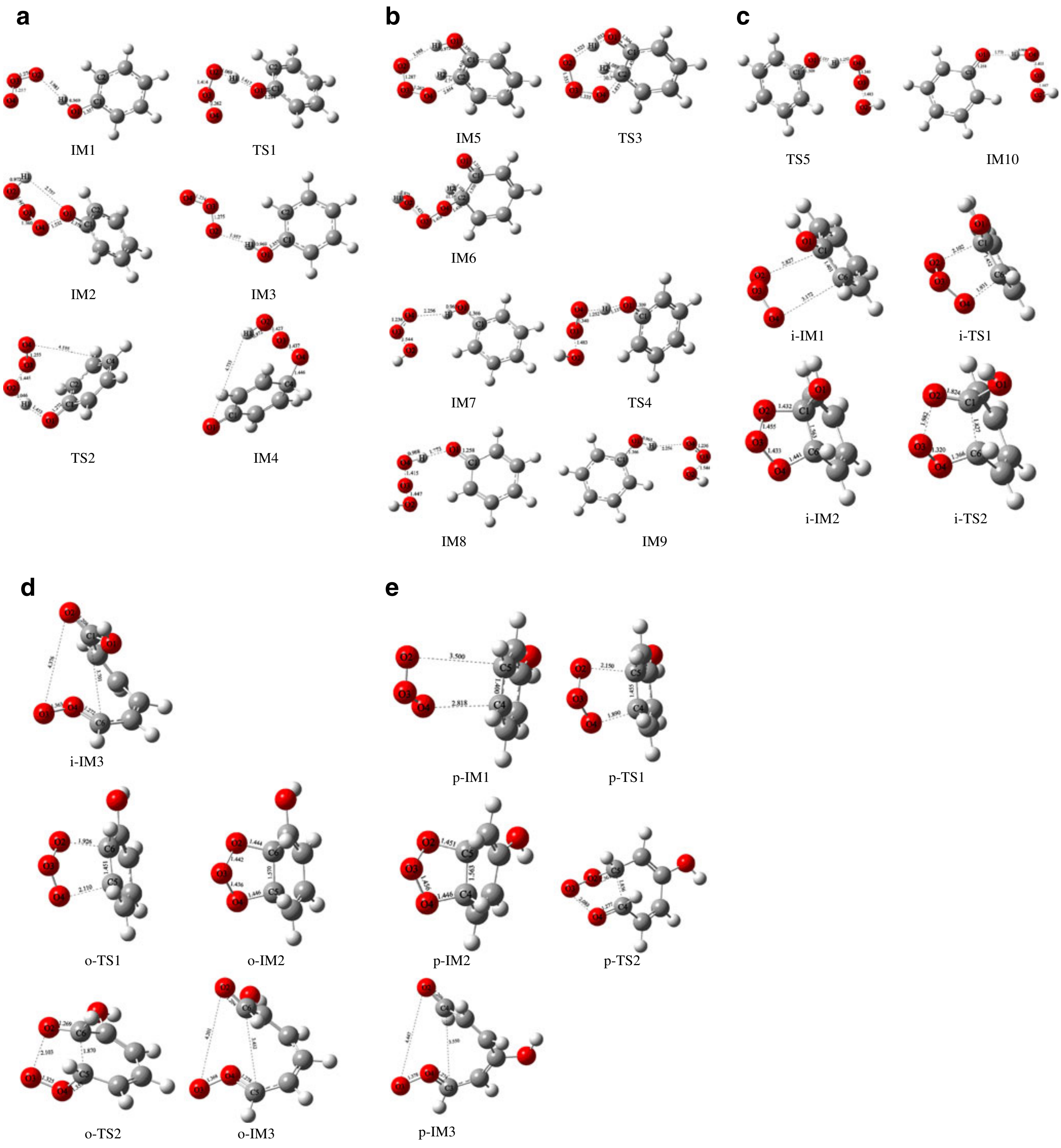

Fig. 3 Optimized geometries of the intermediates and transition states at B3LYP/6-311++G** level (The gray-, white-, red-, and green-balls denote carbon, hydrogen, oxygen, and chlorine atoms, respectively, and bond lengths are in angstroms.)

should be the easiest way to occur. Then one intermediate, IM6, is generated owning a high energy of 22.91 kcal·mol^{-1}. IM6 can react via the cleavage of O3-O4 bond to produce ·HO_2 radical and o-C_6H_5OO· radical (denoted as P3), which can form o-bezenoquinone by further oxidization. Therefore, the pathway of O_3 abstracting phenolic H and adding to ortho- site then forming P3 is the most predominant in the phenolic H abstraction from phenol. According to the experiment of Eisenhauer [29], o-bezenoquinone is one intermediate during the ozonization of phenol. Comparing three O_3 abstracting the phenolic H atom pathways (see Table 3 and Fig. 4) it is found that O_3 abstracting the phenolic H atom and adding to the ortho- site

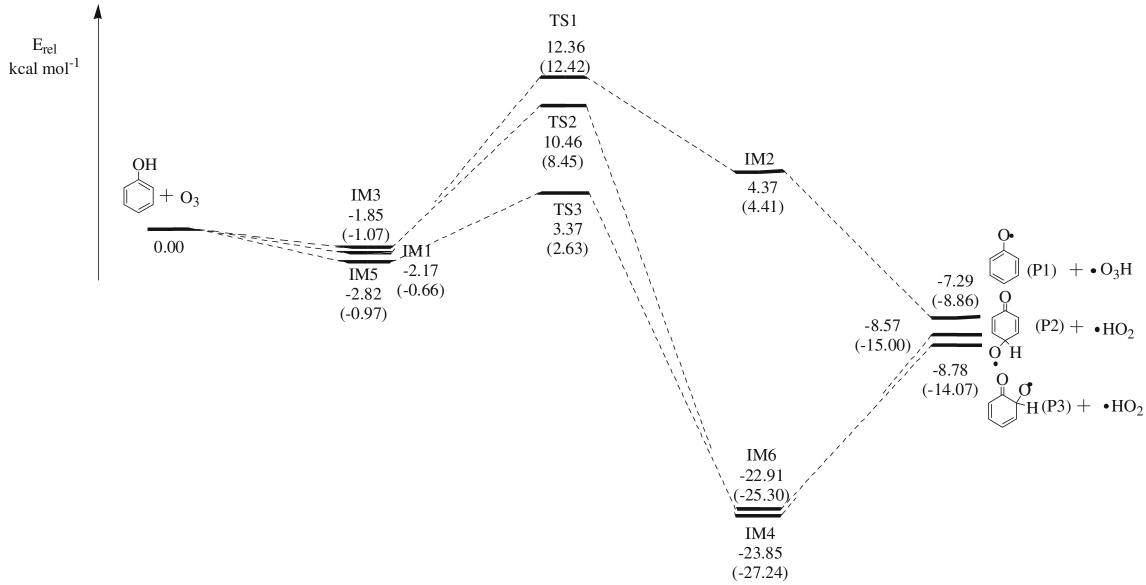

Fig. 4 Calculated potential energy surface profile for the H abstraction reaction of phenol by O_3 at theB3LYP/6-311++G(d,p) level and temperature 298.15 K (the values in parentheses are in the condition of water)

simultaneously (R3) is most energetically favorable, and then the pathway R2 and R1, respectively. It may be the O_3 structure that has difference attack orientation, which induces the reaction occurring through TS3 has the lowest barrier.

It is interesting to compare the three product-like complexes, IM2、IM4 and IM6. In IM2, the leaving $\cdot O_3H$ radical is loosely adhered to the $C_6H_5O\cdot$ radical. However, in IM4 and IM6, the left $\cdot O_3H$ radical adds to the para-C4 and the ortho-C2, respectively. Moreover, the energy of IM2 is 4.37 kcal·mol^{-1} higher than original reactants, but those of IM4 and IM6 are 23.85 kcal·mol^{-1} and 22.91 kcal·mol^{-1} lower than the original reactants, respectively. Probably because the adduct of four oxygen atoms in IM2 connected together is incredibly unstable it leads to the energy of IM2 being much higher than those of IM4 and IM6.

After the three O_3 abstracting the phenolic H atom pathways, the reaction system might have the$\cdot O_3H$ radical. Therefore, the $\cdot O_3H$ radical is active and could possibly react with the phenolic compound. In order to investigate the reaction paths, $\cdot O_3H$ radical abstracting phenolic H atom are also considered, which are illustrated in Scheme 2. It is interestingly noticed that the corresponding intermediates and transition states of the two paths are mirror symmetry (seen in Fig. 3) and the related energies of them are identical (shown in Table 3), so only the R7 pathway needs to be discussed as an instance in detail. A complex, IM7, is formed in a fairly early stage of the reaction, and the energy of it is 1.76 kcal·mol^{-1} more stable than that of the original reactants due to the weak stabilization of the O4…H-O1 hydrogen bond with the distance of 2.256 Å. Then, the transition state TS4, calculated to be 7.92 kcal·mol^{-1} less stable than that of the isolated reactants, is located on the potential energy surface. After that, one adduct, IM8 is formed with the migrating HOOOH loosely being connected with the $C_6H_5O\cdot$ radical. Finally, the decomposition of IM8 yields $C_6H_5O\cdot$ radical and hydrogen trioxide

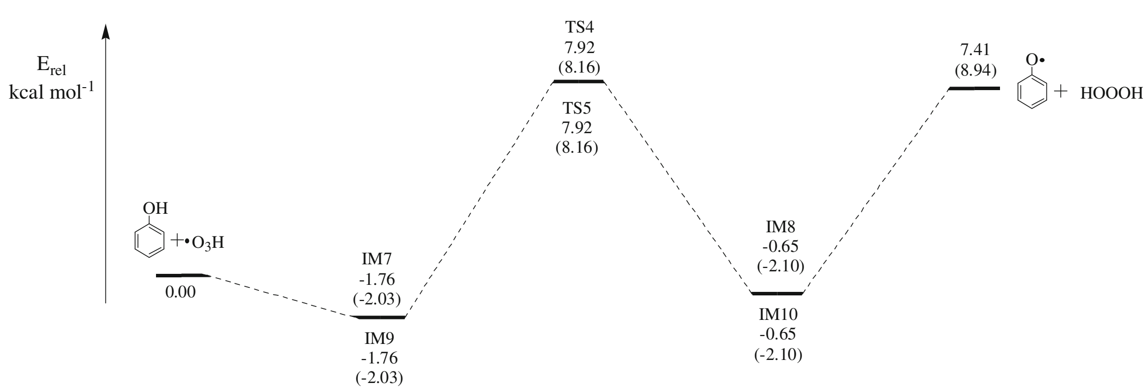

Fig. 5 Calculated potential energy surface profile for the H abstraction reaction of phenol by $\cdot O_3H$ at theB3LYP/6-311++G(d,p) level and temperature 298.15 K (the values in parentheses are in the condition of water)

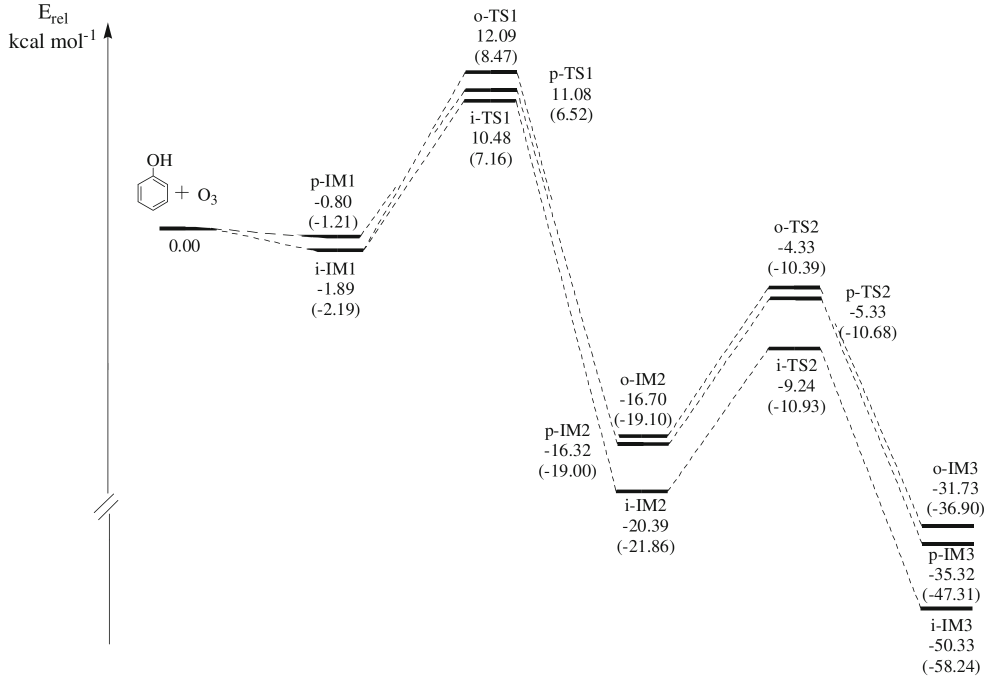

Fig. 6 Calculated potential energy surface profile for the addition reaction of O_3 and phenol at theB3LYP/6-311++G (d,p) level and temperature 298.15 K (the values in parentheses are in the condition of water)

(HOOOH), which is in consonance with the experimental observations [27, 59]. The energy barrier of overall reaction is 9.68 kcal·mol^{-1}, demonstrating that this channel is likely to easily occur.

Cyclo-addition and ring-opening reaction mechanism

All possible situations that O_3 adds to the aromatic ring are taken into account, and we obtain three degradation pathways. First of all, the cyclo-addition of O_3 to the ipso- and ortho- sites (C1 and C6) are considered, and the reaction paths R4a and R4b are found. A pre-reactive complex, i-IM1, of which the energy is 1.89 kcal·mol^{-1} lower than the total energy of original reactants (phenol and O_3), is first located. In i-IM1, the distances between C1 and O2 as well as C6 and O4 are 2.827 Å and 3.172 Å, respectively. Then i-IM2 is formed via a transition state, i-TS1, where the distances between C1 and O2 as well as C6 and O4 are reduced by 25.65% and 39.12%, respectively. IRC calculation indicates that i-TS1 connects i-IM1 and i-IM2. The R4a process has an activation energy of 12.37 kcal·mol^{-1}, and high reaction energy of 20.39 kcal·mol^{-1} is retained in the adduct, i-IM2, which can further react like the R4b path via opening the aromatic ring. As shown in Scheme 1 and Fig. 3, a transition state, i-TS2 is identified along the path R4b. In the i-TS2 structure, the bonds being broken of C1-C6 and O2-O3 are 16.89% and 36.22% longer than the equilibrium value in i-IM2. Finally, the ring-opening product i-IM3 is obtained. The potential barrier of R4b reaction is 11.16 kcal·mol^{-1}, and this process is strongly exothermic by 29.94 kcal·mol^{-1}.

With respect to adding to the ortho- and meta- sites (C6 and C5), reaction paths R5a and R5b are indicated. It is intriguing to notice that the transition state (o-TS1) shares the common pre-complex (i-IM1) with the i-TS1 structure. Along the R5a reaction path, o-IM2 is formed from i-IM1 via the transition state o-TS1, where O2 and O4 atoms of O_3 are adding to C6 and C5 atoms of phenol to form a five-membered ring. This process has an activation energy of 13.98 kcal·mol^{-1}, which is only 1.61 kcal·mol^{-1} higher than the R4a pathway, and the reaction heat is -16.32 kcal·mol^{-1}. The unimolecular

Table 3 Calculated relative energies (kcal·mol^{-1}) for ozone and phenol reactions with the different reaction pathways at theB3LYP/6-311++G(d,p) level and temperature 298.15 K

	ΔE_g [a]	ΔH_g [b]	ΔE_a [c]	ΔH_a [d]
R1	14.53	−7.29	13.08	−8.86
R2	12.31	−8.57	9.52	−15.00
R3	6.19	−8.78	3.60	−14.07
R4a	12.37	−20.39	9.35	−21.86
R4b	11.16	−29.94	10.93	−26.38
R5a	13.98	−16.70	10.66	−19.10
R5b	12.37	−15.03	8.71	−17.80
R6a	11.88	−16.32	7.74	−19.00
R6b	10.99	−19.00	8.32	−28.31
R7	9.68	7.41	10.19	8.94
R8	9.68	7.41	10.19	8.94

[a] Activation energies in gas phase

[b] Reaction enthalpies in gas phase

[c] Activation energies in water

[d] Reaction enthalpies in water

decomposition of o-IM2 occurs via fission of C5-C6 and O2-O3 bonds, yielding a ring-opening product, o-IM3. A transition state, o-TS2, is located in association with the decomposition. In the o-TS2 structure, the C5-C6 and O2-O3 bonds are stretched by 19.11% and 45.84%, respectively. Calculations indicate that the R5b reaction has an energy barrier of 12.37 kcal·mol^{-1} and is exothermic by 15.03 kcal·mol^{-1}. Thus, o-IM3 should be the possible products for the reaction of O_3 adding to the ortho- and meta- sites of phenol. And this ring-open product is in correspondence with the experimental result of Shen et al. [30, 31].

In addition, we analyze the direct addition of O_3 to the para- and meta- sites (C4 and C5), and two channels R6a and R6b are found. In the path R6a, p-IM1, a pre-complex, is converted into p-IM2 via the transition state p-TS1, where O_3 is added to C4 and C5 atoms of the aromatic ring to form a five-membered ring. The activation energy of this process is 11.88 kcal·mol^{-1}, which is the lowest of the three addition pathways. Moreover, the energy of 16.32 kcal·mol^{-1} as internal energy retains in the adduct, p-IM2. Then, the rupture of five-menbered ring in p-IM2 is invoked by the cleavage of C4-C5 and O3-O4 bonds. The transition state p-TS2, with the being ruptured C4-C5 and O3-O4 bonds increased by 18.75% and 43.41%, respectively, is identified as associated with the ring opening. Finally, p-IM3 is yielded. And this R6b process has an energy barrier of 10.99 kcal·mol^{-1}, and the whole reaction is exothermic by 19.00 kcal·mol^{-1}. This ring-opening product is supported by the observed experimental result [30, 31].

According to the reaction potential energy surface profiles it can be assumed the R6a channel of O_3 adding to the para- and meta-sites as the most possible to occur due to its lowest energy barrier. The R4a process of O_3 adding to the ortho- and ipso- sites is easier to occur than the R5a process. These potential energy surface results are in good correspondence with that para-positions have higher reactivity than ipso- and ortho- position by analyzing the frontier orbital theory of phenol [23].

The reaction mechanism of the ozonation of phenol is explored using quantum chemistry methods in the gas phase while some experiments were investigated in aqueous solution. For the purpose of estimating possible solvent dependences on the mechanism, the PCM optimization calculations for all reactants, intermediates and products are performed and the energy results are displayed in Table 3. It is found that though the mechanisms discussed above will not be changed, the calculated energy barriers and reaction enthalpies of the O3 and phenol reaction in water phase are both lower than those in gas phase. This reveals that these reactions are more favorable in the water solvent. Moreover, R5a, R5b, R6a reactions reaction barriers are more influenced by the water solvent than for other reactions, which indicates that the cyclo-addition and ring-opening reaction mechanism is dominant. In addition R3 reaction has the lowest activation energy. However, the activation energies and reaction energies for the two R7 and R8 pathways in water are somewhat higher than those in gas. Maybe the hydrogen bonds between the $\cdot O_3H$ radicals lead to this result. Further studies will be carried out to investigate these phenomena.

Conclusions

In the present investigation, a comprehensive theoretical study of the degradation mechanisms of phenol invoked by ozone is performed by the density functional theory B3LYP method with the 6-311++G (d, p) basis set. The detailed mechanisms of phenolic H atom abstraction and addition to aromatic ring are distinctly elucidated. The pathway of O_3 abstracting the phenolic H atom and then adding to the ortho- position is the most energetically and kinetically favorable process and the dominant product is o-$C_6H_5OO\cdot$ radical. Moreover, the intermediate $\cdot O_3H$ radical abstracting phenolic H atom are also feasible. One important intermediate $C_6H_5O\cdot$ radical which is a crucial precursor for forming the most toxic organic pollutants-PCDD/Fs is determined. Regarding the cyclo-addition and ring-opening reactions, three pathways are found. Of these, the process that O_3 adds to the para- and meta- sites and then opens the ring is slightly easier to occur than the others. The PCM optimization calculations for the reaction of O3 and phenol in water phase show that the calculated energy barriers and reaction enthalpies are lower than those in gas phase, though the degradation mechanisms are not changed. This suggests that these degradation reactions are more favorable in the water solvent.

Acknowledgments This work is supported by a project of Shandong Province Science and Technology Department (No. 2010177) and a Project of Shandong Province Higher Educational Science and Technology Program (No. J09LB08). We also thank China Postdoctoral Science Foundation (No.20090461215 and 20100481303).

References

1. Uberoi V, Bhattacharya S (1997) Toxicity and degradability of nitrophenols in anaerobic systems. Water Environ Res 69:146–156
2. Veeresh G, Kumar P, Mehrotra I (2005) Treatment of phenol and cresols in upflow anaerobic sludge blanket (UASB) processa review. Water Res 39:154–170
3. Kulkarni U, Dixit S (1991) Destruction of phenol from wastewater by oxidation with sulfite-oxygen. Ind Eng Chem Res 30:1916–1920
4. Kujawski W, Warszawski A, Ratajczak W, Porebski T, Capaa W, Ostrowska I (2004) Removal of phenol from wastewater by different separation techniques. Desalination 163:287–296
5. Seredynska-Sobecka B, Tomaszewska M, Morawski A (2005) Removal of micropollutants from water by ozonation/biofiltration process. Desalination 182:151–157

6. Huang C, Shu H (1995) The reaction kinetics, decomposition pathways and intermediate formations of phenol in ozonation, UV/O3 and UV/H2O2 processes. J Hazard Mater 41:47–64
7. Charinpanitkul T, Limsuwan P, Chalotorn C et al (2010) Synergetic removal of aqueous phenol by ozone and activated carbon within three-phase fluidized-bed reactor. J Ind Eng Chem 16:91–95
8. Santos A, Yustos P, Rodriguez S, Garcia-Ochoa F (2006) Wet oxidation of phenol, cresols and nitrophenols catalyzed by activated carbon in acid and basic media. Appl Catal, B 65:269–281
9. Liu H, Liang M, Liu C, Gao Y, Zhou J (2009) Catalytic degradation of phenol in sonolysis by coal ash and H2O2/O3. Chem Eng J 153:131–137
10. Dabrowski A, Podkoscielny P, Hubicki Z, Barczak M (2005) Adsorption of phenolic compounds by activated carbon–a critical review. Chemosphere 58:1049–1070
11. Caizares P, Lobato J, Paz R, Rodrigo M, Saez C (2005) Electrochemical oxidation of phenolic wastes with boron-doped diamond anodes. Water Res 39:2687–2703
12. Turhan K, Uzman S (2008) Removal of phenol from water using ozone. Desalination 229:257–263
13. Lesko T, Colussi A, Hoffmann M (2006) Sonochemical decomposition of phenolevidence for a synergistic effect of ozone and ultrasound for the elimination of total organic carbon from water. Environ Sci Technol 40:6818–6823
14. Gurol M, Vatistas R (1987) Oxidation of phenolic compounds by ozone and ozone+UV radiationa comparative study. Water Res 21:895–900
15. Esplugas S, Giménez J, Contreras S, Pascual E, Rodríguez M (2002) Comparison of different advanced oxidation processes for phenol degradation. Water Res 36:1034–1042
16. Rosenfeldt E, Linden K, Canonica S, Von Gunten U (2006) Comparison of the efficiency of OH radical formation during ozonation and the advanced oxidation processes O3/H2O2 and UV/H2O2. Water Res 40:3695–3704
17. Lin S, Wang C (2003) Ozonation of phenolic wastewater in a gas-induced reactor with a fixed granular activated carbon bed. Ind Eng Chem Res 42:1648–1653
18. Li L, Zhu W, Zhang P, Lu P, Zhang Q, Zhang Z (2007) UV/O3-BAC process for removing organic pollutants in secondary effluents. Desalination 207:114–124
19. Faria PCC, Órfão JJM, Pereira MFR (2006) Ozone decomposition in water catalyzed by activated carboninfluence of chemical and textural properties. Ind Eng Chem Res 45:2715–2721
20. Gurol M, Singer P (1982) Kinetics of ozone decompositiona dynamic approach. Environ Sci Technol 16:377–383
21. Bremner D, Burgess A, Houllemare D, Namkung K (2006) Phenol degradation using hydroxyl radicals generated from zero-valent iron and hydrogen peroxide. Appl Catal, B 63:15–19
22. Ning B, Graham NJD, Zhang Y (2007) Degradation of octylphenol and nonylphenol by ozone - Part IDirect reaction. Chemosphere 68:1163–1172
23. Morales-Roque J, Carrillo-Cárdenas M, Jayanthi N, Cruz J, Pandiyan T (2009) Theoretical and experimental interpretations of phenol oxidation by the hydroxyl radical. J Mol Struct (THEOCHEM) 910:74–79
24. Lundqvist M, Eriksson L (2000) Hydroxyl radical reactions with phenol as a model for generation of biologically reactive tyrosyl radicals. J Phys Chem B 104:848–855
25. Namkung K, Burgess A, Bremner D, Staines H (2008) Advanced Fenton processing of aqueous phenol solutionsa continuous system study including sonication effects. Ultrason Sonochem 15:171–176
26. Eisenhauer H (1964) Oxidation of phenolic wastes. J Water Pollut Control Fed 36:1116–1128
27. Plesničar B, Tuttle T, Cerkovnik J, Koller J, Cremer D (2003) Mechanism of formation of hydrogen trioxide (HOOOH) in the ozonation of 1, 2-diphenylhydrazine and 1, 2-dimethylhydrazineAn experimental and theoretical investigation. J Am Chem Soc 125:11553–11564
28. Manojlovic D, Ostojic DR, Obradovic BM, Kuraica MM, Krsmanovic VD, Puric J (2007) Removal of phenol and chlorophenols from water by new ozone generator. Desalination 213:116–122
29. Eisenhauer H (1968) The ozonization of phenolic wastes. J Water Pollut Control Fed 40:1887–1899
30. Shen Y, Lei L, Zhang X, Zhou M, Zhang Y (2008) Effect of various gases and chemical catalysts on phenol degradation pathways by pulsed electrical discharges. J Hazard Mater 150:713–722
31. Hoeben W, Veldhuizen E (2000) The degradation of aqueous phenol solutions by pulsed positive corona discharges. Plasma Sources Sci Technol 9:361–365
32. Zhang Q, Qu X, Wang W (2007) Mechanism of OH-initiated atmospheric photooxidation of dichlorvos:a quantum mechanical study. Environ Sci Technol 41:6109–6116
33. Frisch MJ, Trucks GW, Schlegel HB et al (2004) Gaussian 2003. Revision D.01. Gaussian Inc, Wallingford, CT
34. Zhao Y, Truhlar DG (2008) How well can new-generation density functionals describe the energetics of bond-dissociation reactions producing radicals? J Phys Chem A 112:1095–1099
35. Lozynski M, Rusinska-Roszak D, Mack HG (1998) Hydrogen bonding and density functional calculationsthe B3LYP approach as the shortest way to MP2 results. J Phys Chem A 102:2899–2903
36. Lee C, Yang W, Parr R (1988) Development of the Colle-Salvetti correlation-energy formula into a functional of the electron density. Phys Rev B 37:785–789
37. Becke AD (1993) Density-functional thermochemistry III The role of exact exchange. J Chem Phys 98:5648–5652
38. Fukui K (1981) The path of chemical reactions-the IRC approach. Acc Chem Res 14:363–368
39. Gonzalez C, Schlegel H (1990) Reaction path following in mass-weighted internal coordinates. J Phys Chem 94:5523–5527
40. Pauling L (1960) The nature of the chemical bond. in. Cornell University Press, Ithaca, NY
41. Pakiari AH, Nazari F, Weinhold F (2003) The study of relationship between chemical geometry and electronic configuration of non-Walsh systems. J Mol Struct (THEOCHEM) 629:77–81
42. Linnett J (1964) The electronic structure of moleculesa new approach. Methuen London
43. Pakiari A, Nazari F (2003) New suggestion for electronic structure of the ground state of ozone. J Mol Struct THEOCHEM 640:109–115
44. Fujimoto H (1997) Frontier orbitals and reaction pathsselected papers of Kenichi Fukui. World Scientific, Singapore Inc
45. Fleming I (1976) Frontier orbitals and organic chemical reactions. Wiley, New York
46. Vleeschouwer FD, Speybroeck VV, Waroquier M, Geerlings P, Proft FD (2008) An intrinsic radical stability scale from the perspective of bond dissociation enthalpies:a companion to radical electrophilicities. J Org Chem 73:9109–9120
47. de Heer MI, Korth H-G, Mulder P (1999) Poly methoxy phenols in solution O−H bond dissociation enthalpies, structures, and hydrogen bonding. J Org Chem 64:6969–6975
48. Yamada S, Naito Y, Takada M, Nakai S, Hosomi M (2008) Photodegradation of hexachlorobenzene and theoretical prediction of its degradation pathways using quantum chemical calculation. Chemosphere 70:731–736
49. Ren X, Sun Y, Zhu L, Cui Z (2010) Theoretical studies on the OH-initiated photodegradation mechanism of dicofol. Comput Theor Chem 963:365–370
50. Suegara J, Lee BD, Espino MP, Nakai S, Hosomi M (2005) Photodegradation of pentachlorophenol and its degradation pathways predicted using density functional theory. Chemosphere 61:341–346
51. Lim DH, Lastoskie CM (2009) Density functional theory studies on the relative reactivity of chloroethenes on zerovalent iron. Environ Sci Technol 43:5443–5448

52. Zhao Y, Zhang R, Wang H, He M, Sun X, Zhang Q, Wang W, Ru M (2010) Mechanism of atmospheric ozonolysis of sabineneA DFT study. J Mol Struct (THEOCHEM) 942:32–37
53. Denisova T, Denisov E (1998) Reactivity of ozone as a hydrogen-atom acceptor in reactions with antioxidants. Polym Degrad Stab 60:345–350
54. Janoschek R, Fabian W (2003) Thermodynamic properties of chlorinated phenols, cyclo-C5 compounds, and derived radicals from G3MP2B3 calculations. J Mol Struct 661:635–645
55. Berho F, Lesclaux R (1997) The phenoxy radicalUV spectrum and kinetics of gas-phase reactions with itself and with oxygen. Chem Phys Lett 279:289–296
56. Asatryan R, Davtyan A, Khachatryan L, Dellinger B (2005) Molecular modeling studies of the reactions of phenoxy radical dimersPathways to dibenzofurans. J Phys Chem A 109:11198–11205
57. Altarawneh M, Dlugogorski BZ, Kennedy EM, Mackie JC (2009) Mechanisms for formation, chlorination, dechlorination and destruction of polychlorinated dibenzo-p-dioxins and dibenzofurans (PCDD/Fs). Prog Energy Combust Sci 35: 245–274
58. Asatryan R, Davtyan A, Khachatryan L, Dellinger B (2002) Theoretical study of open-shell IPSO-addition and bis-keto dimer interconversion reactions related to gas-phase formation of PCDD/FS from chlorinated phenols. Organohalogen Compd 56:277–280
59. Plesničar B, Cerkovnik J, Tekavec T, Koller J (1998) On the mechanism of the ozonation of isopropyl alcohol:an experimental and density functional theoretical investigation 17O NMR Spectra of hydrogen trioxide (HOOOH) and the hydrotrioxide of isopropyl alcohol. J Am Chem Soc 120:8005–8006